

Modal Characteristic Analysis of an Alouette Rotor Blade

a project presented to
The Faculty of the Department of Aerospace Engineering
San José State University

in partial fulfillment of the requirements for the degree
Master of Science in Aerospace Engineering

by

Jeremy Untalan

December 2018

approved by

Dr. Jeanine Hunter
Faculty Advisor



San José State
UNIVERSITY

Modal Characteristic Analysis of an Alouette Rotor Blade

Jeremy Untalan

San Jose State University, San Jose, CA, 95192

Simulation is a strong tool that engineers today are taking full advantage of. It provides the flexibility of changing design parameters on the fly without using financial resources necessary to go to a full-scale model for testing. Finding the modes of a structure is important when designing new system because it is important to avoid situations like the Tacoma Narrows Bridge incident of 1940 where there was catastrophic failure due to harmonic resonance. This paper attempts simulate the modes of an Alouette rotor blade through two approaches. The first approach is through a MATLAB script that uses Euler Bernoulli beam theory and the second approach is through an ANSYS simulation. The simulations are then verified against actual modal test data.

Nomenclature

CAD	=	computer aided design
FEA	=	finite element analysis
FEM	=	finite element model
\vec{F}	=	force
m	=	mass
\vec{a}	=	acceleration
J	=	torsional constant
G	=	shear modulus
q_i	=	coordinates
ANCF	=	absolute nodal coordinate formulation
M	=	mass matrix
K	=	stiffness matrix
\ddot{U}	=	acceleration matrix
F	=	applied forces matrix
UUT	=	unit under test
TC	=	test conductor
FRF	=	frequency response function
DAS	=	data acquisition system
$PSMIF$	=	power spectral mode indicator functions

I. Introduction

A. Motivation

WHENEVER a new aerospace system is being designed, it must undergo extensive testing. This is due to the very nature of aerospace engineering. The systems that are designed are expensive and allow zero margin for error due to their payloads. For a satellite, which could cost upwards of \$300 million, the payload could be new scientific research instrumentation, military applicable sensors, or even commercial connectivity for a nation. For an aircraft, the payload is far more valuable as it deals with human life.

Due to the heavy price, it is imperative that precautions be taken to alleviate potential dangers. One of the dangers is resonance at the natural frequency of the dynamic system which would produce catastrophic damage. One of the most famous examples is the Tacoma Narrows Bridge incident of 1940 where the wind put enough of an input that it resonated with the bridges natural frequency, causing it to collapse the same year it was built. To circumnavigate this issue, when designing and manufacturing aerospace systems, dynamicists investigate the mode shapes of subsystems in order to avoid creating a system that resonates and produce another incident like the Tacoma Narrows Bridge collapse.

B. Literature Review

1. *Simulation*

With the advancement of technology, engineers have new tools to design these systems using more extensive research and development. Computer Aided Design has opened up a new field of engineering that allows designers to build and modify systems using far fewer resources. Using CAD models as a starting point, a transformation method is applied to produce a discreet structure that is represented by a finite number of easily expressed elements that are connected by finite

nodes for Finite Element Analysis (FEA)¹. First, a step is taken to express the system in a usable form for FEA. The model needs to be geometrically parametrized, so features can be represented by a description or simplified representation. In mathematics, parametrization is the specification of an object such as curve or surface by a single variable given a specific range. The benefit of this is that a geometry can be described with a minimum number of parameters which increases smoothness while maintaining enough information. The reason that this is important is because it reduces the computational time and power to analyze the specimen. Once this is done, a mesh can be generated over the model to produce something usable for numerical methods. An example can be seen in Fig. 1. The mesh

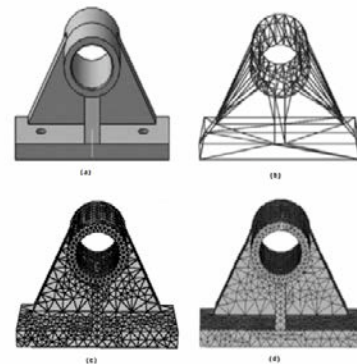


Fig. 1 Geometric Idealization example¹.

can be auto generated or modified to perform efficiently, depending on the user's goal. When running a simulation, it is important to properly manage the available resources. From Fig 1, it is apparent that there is a more concentrated mesh around eye hole of the bracket. There are few reasons for this: First, because of the shape of the elements, it is hard to model a circular shape using a linear element. Second, and more important, regions of stress concentration or high stress gradients due to fillets, holes, or re-entrant corners require a finer mesh near those regions¹⁷. A stress concentration is a location where stress is focused. An object is stronger when force is evenly distributed over its area, so any reduction in area such as a hole can result in a localized increase of in stress.

There are two different types of meshing: structured and unstructured. Structured means that the cells and grid lines are layered in an orderly fashion throughout the domain. An unstructured

mesh is the opposite where the cells are laid in an arbitrary fashion, which is great for complex shapes, but requires much more computational power.

Once the model has been produced, a Finite Element Model (FEM) approach will be implemented. FEM is a numerical technique to find approximate solutions to problems through the use of linear/partial differential equations. Further simplifications and assumptions may need to be done in order to get a high fidelity model of the specific situation. An example is modeling a flexible wing structure. For this problem, the Euler-Bernoulli beam theory is utilized so that small displacements and linear elastic material can be considered. This is the technique used in this paper².

2. Modeling

Dynamic modeling is used to describe how a system will respond or move when acted upon by forces³. Using Newton's second law of motion (seen in Equation (1) where Force, \vec{F} , equals mass, m , times acceleration, \vec{a}) as a basis, equations of motion can be derived. The equations of motion allow us to understand the dynamic behavior of a system.

$$\sum \vec{F} = m\vec{a} \quad (1)$$

For an element, a stiffness matrix $[k]$ and mass matrix $[m]$, relate the nodal displacement, $[u]$, and accelerations $[\ddot{u}]$ to the nodal forces¹⁷. These problems area all governed by the following 1-D differential equation:

$$\frac{d}{dx} \left(k \frac{du}{dx} \right) + f = 0 \quad (2)$$

Using FEM, we can convert this differential equation into a system of algebraic equations:

$$[M][\ddot{U}] + [K][U] = [F] \quad (3)$$

There are two methods employed to handle the flexible body dynamics. One is where the overall assembly is broken up into reduced models with imposed reduced degrees of freedoms limited to the interfacing nodes⁵. Such is the case when spacecraft companies deliver a simplified component mode synthesis to launch vehicle companies for them to run their own transient simulations. These simplified models, while acceptable for smaller sized launch vehicles, proved to not be accurate enough to predict a larger launch vehicles input into the spacecraft's FEM resulting in unanticipated excitations⁵. While trying to keep detailed information, this method can be divided up into large number of elements. However, in order to retain these large matrices and provide any meaningful analysis, the amount of resources necessary may not be available. The second method uses a “branch-modes” technique that has imposed limits that make an assumption that the boundary between the two separate sub models needs to be rigid⁶. In each method, there have been a more enhanced approaches in current years^{5,6}.

Recently, there has been a new proposed formulation called the Absolute Nodal Coordinate Formulation (ANCF)⁷. Using ANCF, the rigid body is described in the Newtonian frame rather than the body frame. Then the fully parameterized body elements can be used for the complete description of the beam and cross-sectional deformations. An example can be seen in Fig. 2. Further work has been done such as optimization, model order reduction, and Absolute Nodal Coordinate Formulation- Reference Node^{8,9,10}

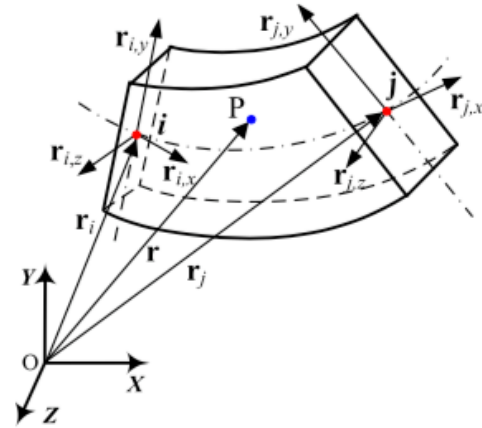


Fig. 2 Absolute Nodal Coordinate Formulation reference frame.

3. Modal Analysis

One reason that FEM is important is because it can be used to determine the characteristic frequency, also known as the natural frequency of the system. All stable, unforced, mechanical systems resonate at certain discrete frequencies¹¹. This means that any input that is introduced at this frequency will be amplified. So, if a system has an applied time-varying force at the structure's natural frequency, it will cause a large response that may be harmful to the system as a whole. Sometimes a system has several natural frequencies such that each frequency correlates to a mode of vibration. When found, these mode shapes can provide insights to how that subsystem would affect

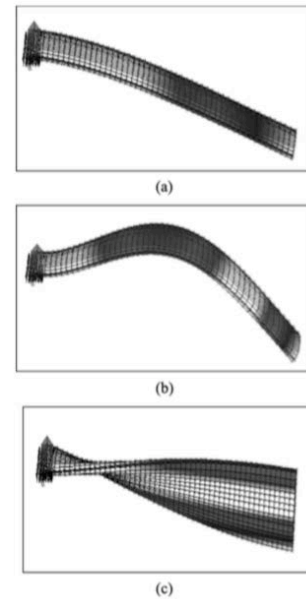


Fig. 3 This shows a displacement modes derived from the FEM. (a) and (b) are both bending modes, while (c) is a torsional mode.

the connecting subsystems. It might induce a torsional twist, rocking, or bending mode. Figure 3 shows an exaggerated numerical simulation found using the FEM.

These numerical results can be validated through dynamic system testing. Normally, when testing large systems, the natural frequency of the system have been simulated and verified. Going down into the subsystem level, modal testing is done early in the design phase. This allows enough time for the engineers to make a decision early enough if required. If the predicted modes are nowhere near the test results, it could possibly require a complete redesign if serious enough. There are generally three test methods used to validate the mode shapes. All methods require the use of an excitation force, which can range from a shaker, a hammer, or a combination of both. As long as it is possible to excite all axes and acquire clean data, any method can be used. As stated earlier, the first to be considered is a tap test. Using a calibrated hammer with a rubber tip, it is possible

to hit the test article with enough force to excite the accelerometers. If that is not enough, one or two shakers can be used to excite the test article to get the required data. The shakers, which operate on the same principles of a speaker, vibrate either randomly or through sine wave sweeps. With a random vibration signal, it is a statistical approach to a structures response to a given random environment. A sine signal input is an input that provides a predictable, regular sine wave oscillation. Since it is more structured, it is possible to measure any frequency and determine the acceleration of any point on the FEM. Once the data has been acquired, a Bode plot can be generated. If the software with the appropriate capabilities is available, the dynamicists would be able to overlay the specific accelerometer axis on top of each other and validate the mode shapes. Using the same software, it would be possible to impose the data of the dynamic response and animate the FEM to have a visual representation

C. Project Proposal

The objective of this project is to create an accurate mathematical model of a flexible helicopter rotor blade segment and to verify it. The verification process will subject the test article to an outside excitation force using a shaker and accelerometers attached to various locations in order to capture real time data for analysis. This project will identify the different modes shapes and what to expect from the test article such as rocking in different axis and/or torsional twisting.

D. Methodology

This project will use Newton's Law of Motion to generate the mathematical model of the rigid body structure. Using MATLAB, the system will be subjected to an impulse input and an analysis

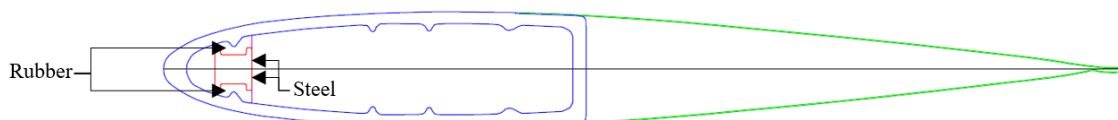


Fig. 4 Modified NACA0012 airfoil used as a template for the CAD model in PTC Creo¹³.

will be performed. PTC Creo will also be used for further validation of the MATLAB code using its finite element analysis. Finally, the unit will be manufactured and tested using a shaker and accelerometers and gathered via a data acquisition system. The testing system will use NX Test For I-DEAS software and AFPoly to validate the modal frequencies derived from the simulations. Using Test For I-DEAS, the CAD model will then be animated to show an exaggerated motion of the different mode shapes.

II. Simulation

A. FEA

1. Set Up

The unit was modeled after an Alouette rotor blade. The model was based on a modified NACA0012 airfoil that had a 16" chord length based off of figure 4. The conventional rotor blade is broken up into one subassembly, the strut, and a separate single part, the airfoil. The strut subassembly is further broken down into four different parts that consist of the core. Two parts of the core are the rubber bits that wedge the other two parts, which is steel, located on the forward section of the rotor blade. The assembly has a total of 5 parts. The assembly is then imported into ANSYS where the material properties were imposed and the global coordinates were generated. The model is based off the Cartesian coordinate system with the origin located at $\vec{r} = 0.0\hat{i} - 0.0\hat{j} + 0.0\hat{k}$ meters off the center of the fixed base of the rotor blade. Fig.

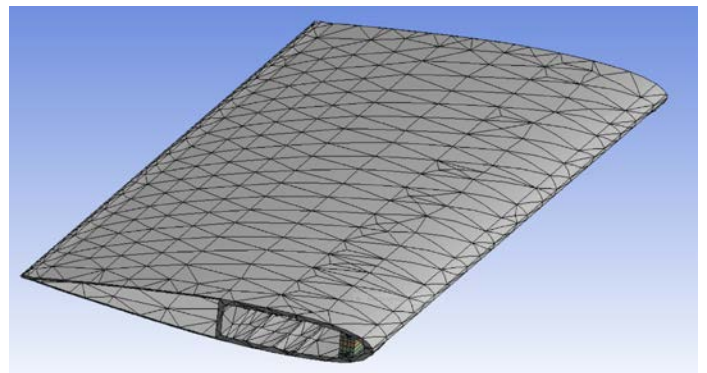


Fig. 5 Unstructured mesh generated by ANSYS.

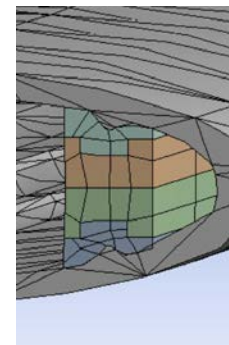


Fig. 6 Closer look at the mesh generated for the core.

7 shows the cartesian coordinate system used across all simulations. The next step was to define the contact type to 'bonded' on all the connecting faces between the parts. The model was then meshed using an element size of .02m. The mesh was automatically generated by the program. It resulted in an unstructured grid due to the shape of the airfoil and the grid employs a combination of tetrahedrons and pyramids for the 3D model. A closer look can be found in Fig. 4 and Fig 5. For the modal analysis, a fixed support environment was applied to one end of the 72-inch blade to simulate the test environment. There is no applied load because when performing a modal analysis, the geometry is the only thing that affects the resonating frequencies. The simulation was run looking for modes in the frequency range of 0-600 Hz as defined in MIL-STD810F, Table 514.5C-IV¹⁴.

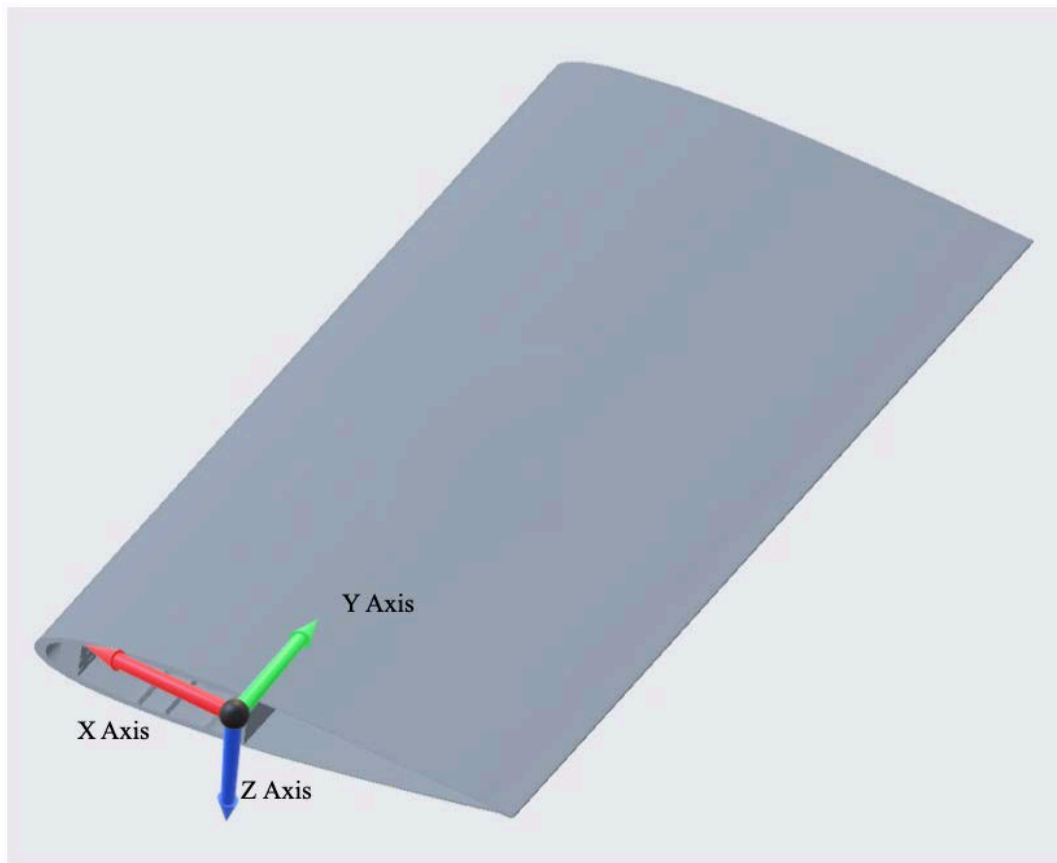


Fig. 7 Axis defined for ANSYS. X axis is pointed towards the leading edge of the airfoil, Y axis is pointed down the airfoil length, and Z axis towards the bottom of the airfoil.

2. Results

In an FEA model, the solver is basically solving the spring equation seen in Equation (4). The model is solved in matrix form because it is broken into tiny elements and these tiny elements are discretized and act as tiny springs with a local stiffness matrix. A local stiffness matrix is built for each element then a global stiffness matrix is imposed over the whole model by combining the individual element stiffness matrices. Applying the boundary conditions, the force and stiffness matrices are known, allowing the simulation to implement its extraction method to find the displacements. Calculating these natural frequency and mode shapes is at its core an eigenvalue problem. It is assumed that the model is symmetrical and there is no damping. ANSYS has four different extraction methods that it can use to solve for modal analysis. Each method has scenarios that would bring about the optimal results and has a very specific application. The first solver is the Block Lanczos Method which is the default solver¹⁵. It is used to find 40 plus modes of a large model. It is especially useful when the model consists of poorly shaped solid and shell elements. It performs particularly well when the model is made up of just shells or a combination of shells and solids and requires a medium amount of memory but a low amount of disk space. The second method is the Subspace Method¹⁵. The Subspace Method was popular in the earlier years since it did not require much memory but did require a high amount of disk space. It worked well at finding a few nodes of small models fairly quickly. However, as the models become more complex and larger, the solution time naturally increases. The third solver is the Reduced Method, which is an older eigen solver, that reduces matrices in order to minimize the number of dynamic degrees of freedom¹⁵. It requires a low amount of memory and a low amount of disk space. It is useful to find the modes of small to medium models that have less than 10,000 degrees of freedom. It is

limited because it can only find up to 40 modes of larger models and that is dependent of the user selected master Degree-of-Freedom. The master Degree-of-Freedom is chosen to represent the dynamic response of the system and needs to be chosen as accurately as possible. The last eigen solver is the Power Dynamics Method, which is based off the Subspace Method but uses the Preconditioned Conjugate Gradient Solver (also known as PCG-Solver)¹⁵. It is great for large models with up to 10,000,000 degrees of freedom at a reasonable solution time and can find up to 100 modes. It performs well when the model is a well-shaped 3D solid element, similar to static or full transient analysis. Naturally, it requires a high amount of memory required but a low amount of disk space. With coarse mesh models, the frequencies are accurate but there is a possibility of missed modes due to repeating frequencies. For this model the Block Lanczos Method was implemented because the model imported in PTC Creo might have been transferred into ANSYS using a combination of shells and solids. The simulation was then run with the results show in in Table 1 and Figures 8-17. The results shown are the amount of displacement with red indicating the maximum displacement. Figure 8 shows the wireframe of the unperturbed airfoil superimposed upon the mode shape of that correlating frequency.

Table 1 ANSYS results for Alouette rotor blade

<u>Mode</u>	<u>Frequency (Hz)</u>	<u>Axis of Rotation</u>
1	15.34	X
2	92.25	X
3	97.446	Z
4	125.09	Y
5	244.05	X
6	348.09	Y
7	443.62	X
8	488.35	Z
9	528.24	Y

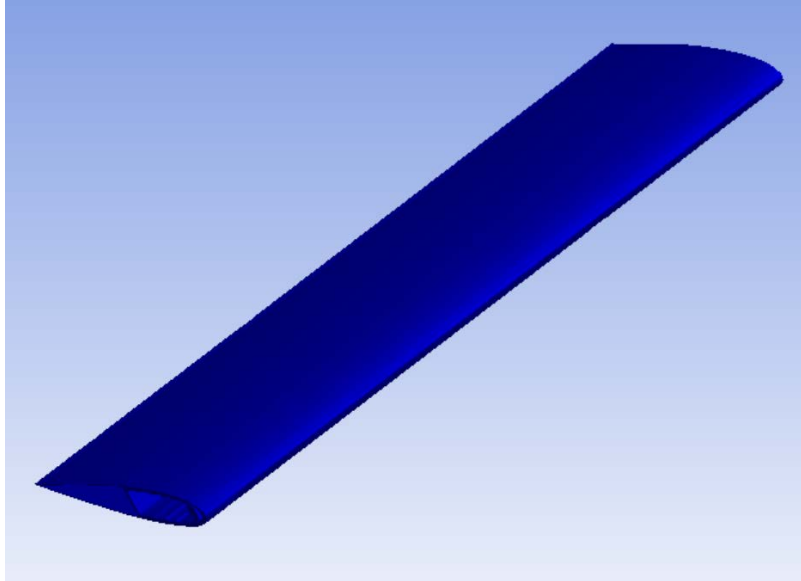


Fig. 8 Undeformed Alouette Rotor Blade

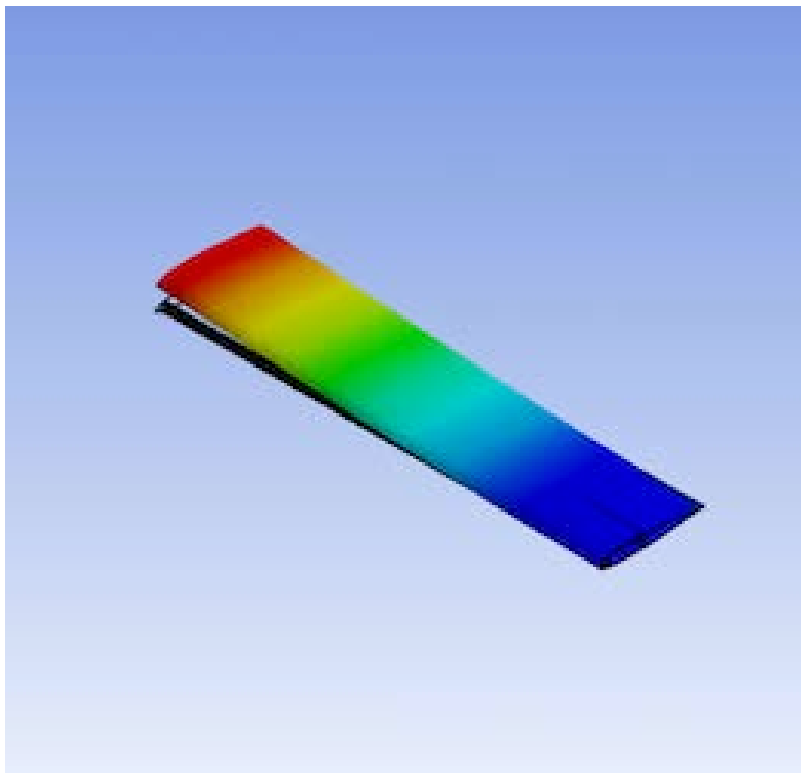


Fig. 9 First mode shape at 15.35 Hz

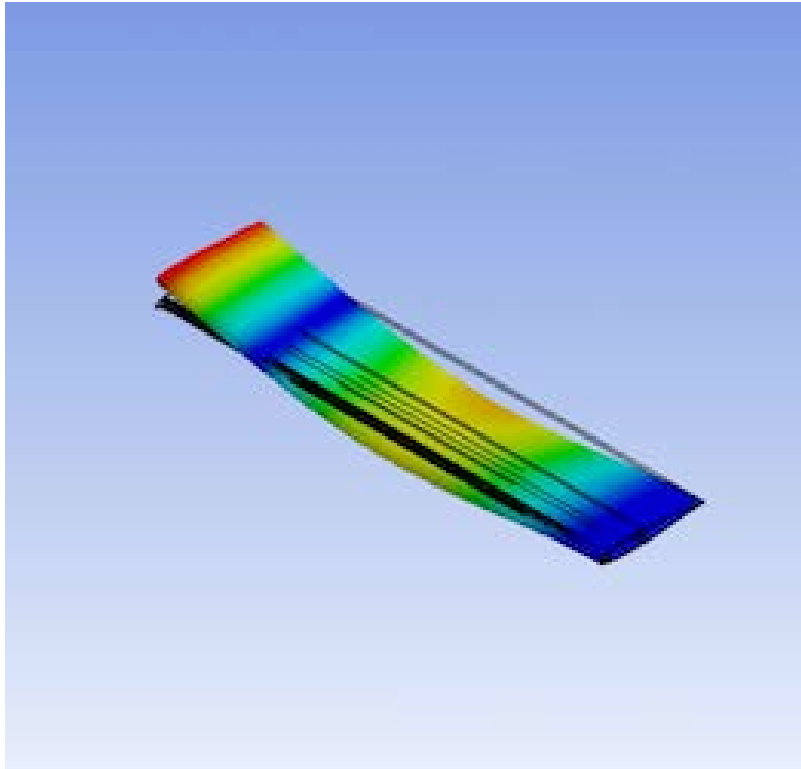


Fig. 10 Second mode shape at 92.25 Hz

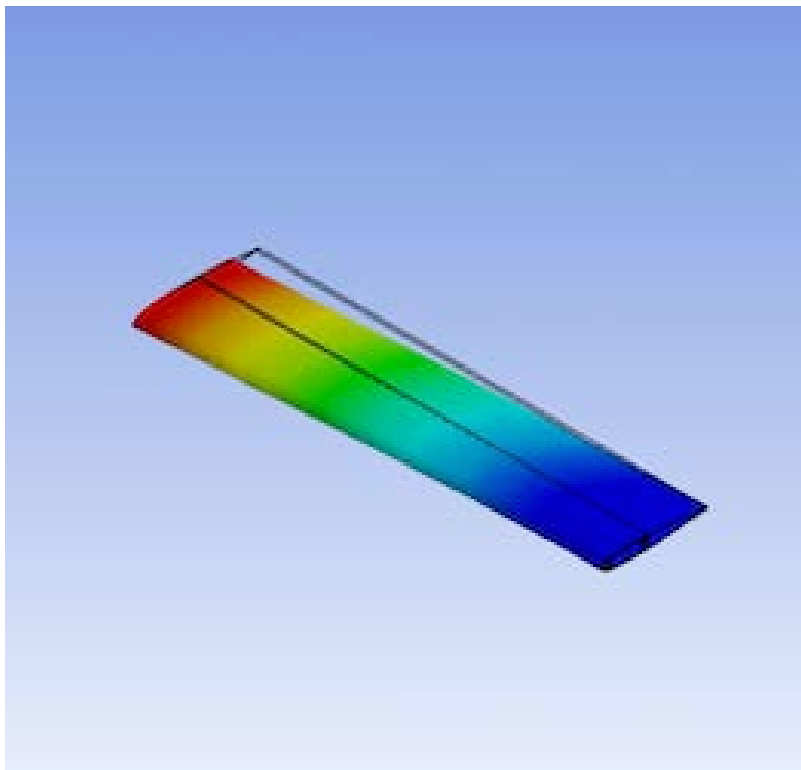


Fig. 11 Third mode shape at 97.45 Hz

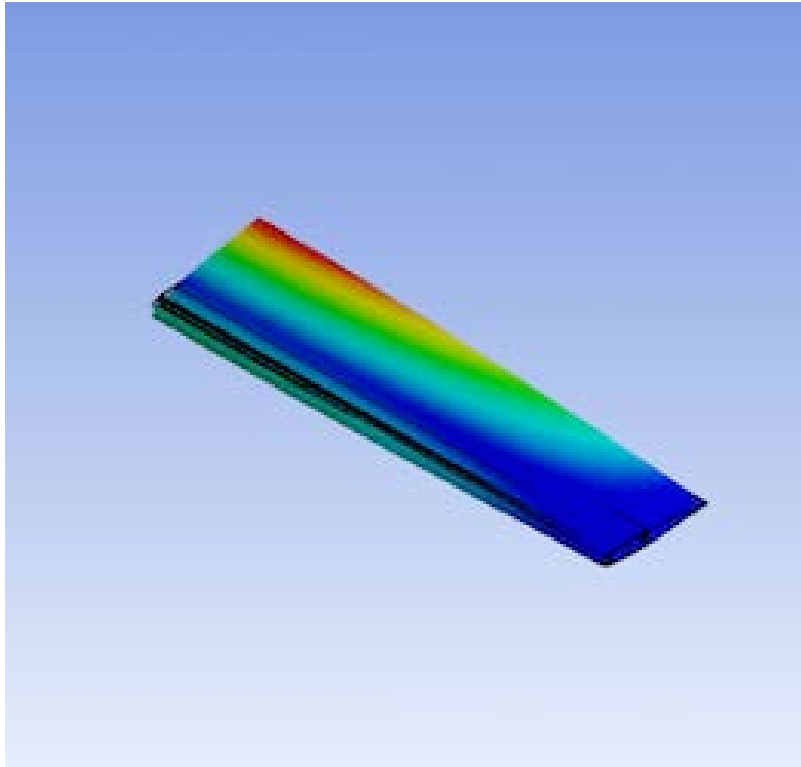


Fig. 12 Fourth mode shape at 125.09 Hz

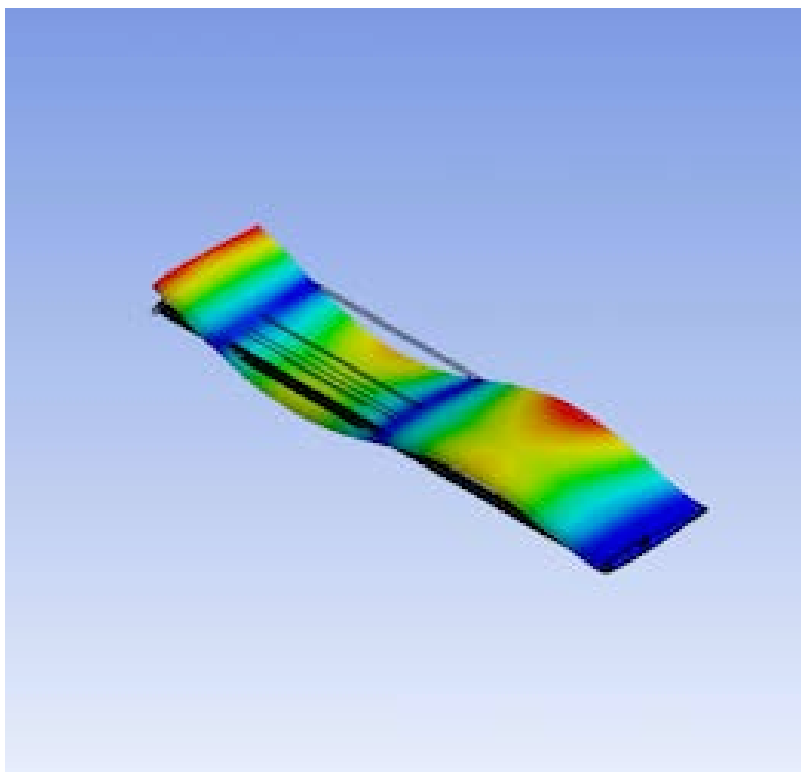


Fig. 13 Fifth mode shape at 244.05 Hz

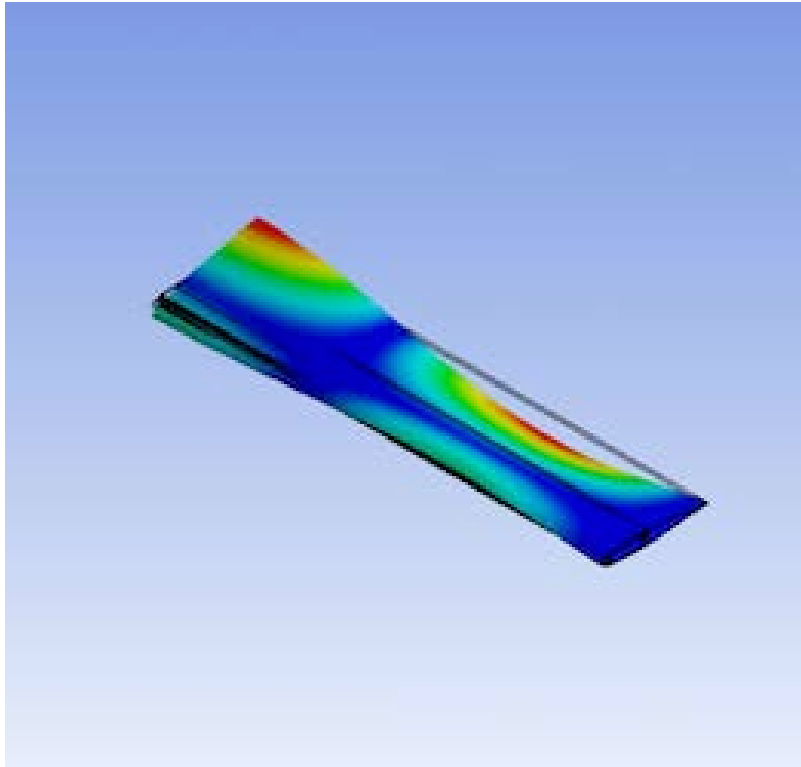


Fig. 14 Sixth mode shape at 348.09 Hz

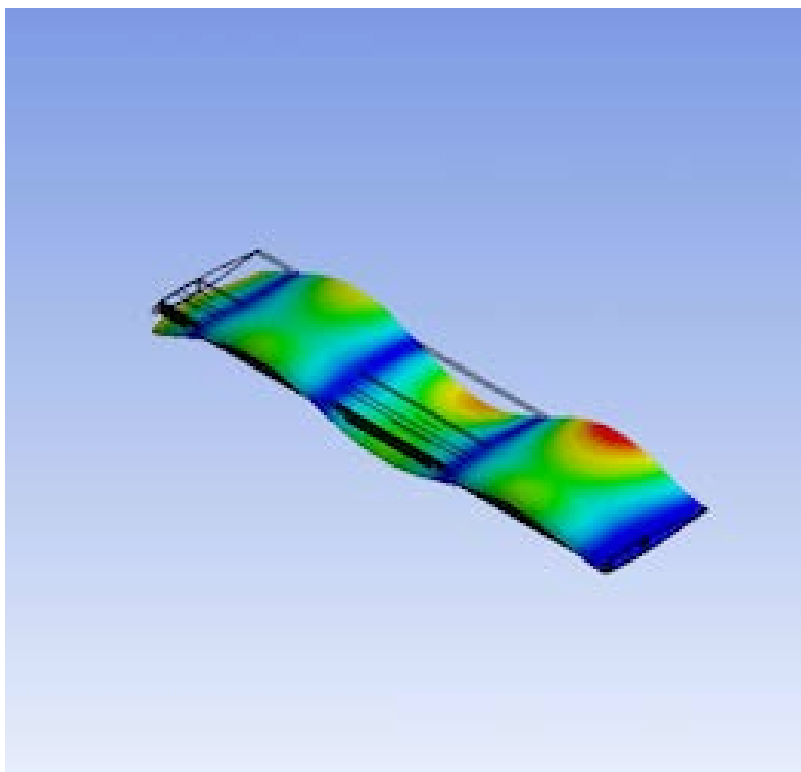


Fig. 15 Seventh mode shape at 443.62 Hz

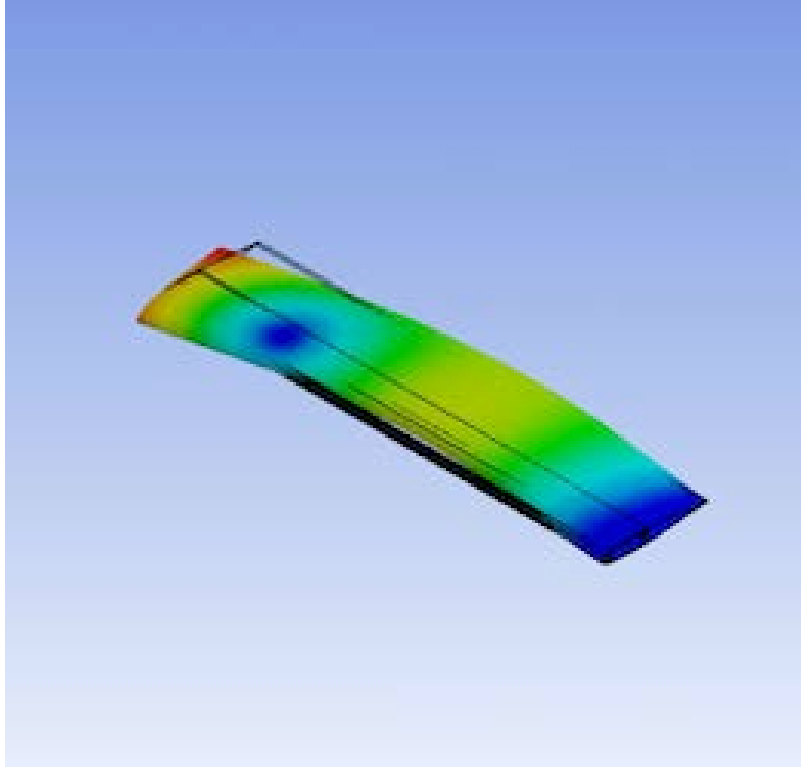


Fig. 16 Eighth mode shape at 488.35 Hz

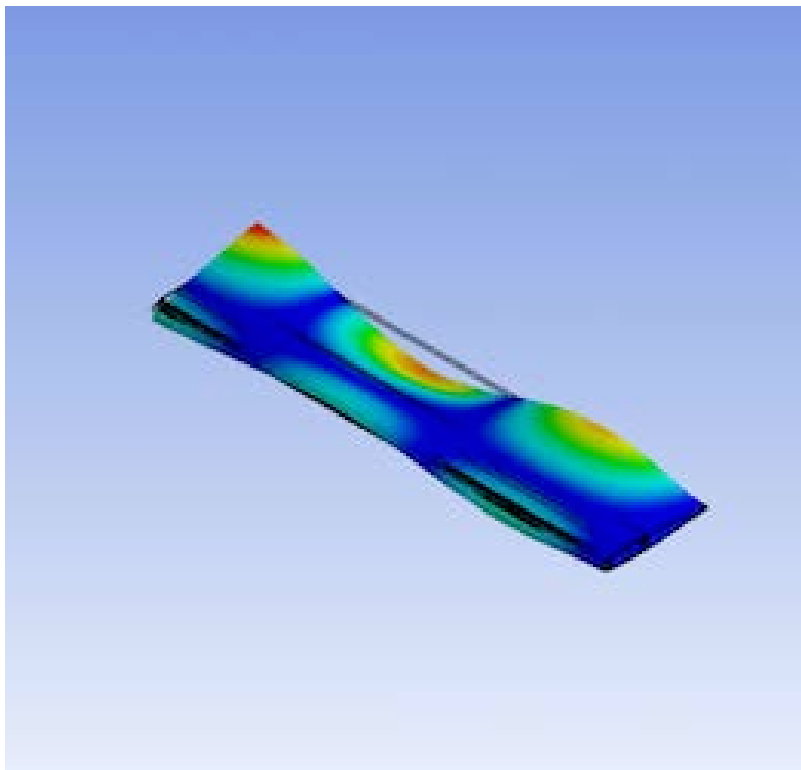


Fig. 17 Ninth mode shape at 528.24 Hz

The first mode shape simulated was the first bending mode at 15.35 Hz. There is only one node, which was where the test specimen was placed as a fixed support. A node is a place where there is minimal displacement along the test article. The second mode shape was found at a higher frequency at 92.25 Hz. This was still about the X axis, however, there were two nodes. The third mode shape was not too far off and was found at 97.45 Hz. This mode shape had one node, similar to the first mode. Unlike the first mode, this one was about the Z axis. The fourth natural frequency found is another singular node mode shape about the Y axis at 125.09 Hz. The fifth and seventh are also about the X axis at 244.05 Hz and 443.62 Hz with third and fourth node added respectively. The sixth and ninth modes were about the Y axis at 348.09 Hz and 528.24 Hz with a second and third node added, similar to the X axis mode shapes. Finally, the eighth mode shape was found at 388.35 and is the second mode shape about the Z axis with two nodes.

B. MATLAB Simulation

1. Equation of Motion for Finite Element Methods

In order to better understand what ANSYS is doing, a MATLAB code was written to verify the simulation results. Finite Element Methods is a way to determine mode and mode shapes. In order to accomplish this, the mass, M , and stiffness, K , matrices need to be generated. The corresponding displacement and accelerations for these degrees of freedom are contained the matrices \ddot{U} and U . The applied forces are contained in the force matrix F . The resulting undamped equation of motion for the free unconstrained structure is:

$$[M][\ddot{U}] + [K][U] = [F] \quad (4)$$

2. Variable Definition

The material being used is 'aluminum', which was used as the material of the airfoil shell in ANSYS. The following parameters were defined in the ANSYS model: $E = 7.1 * 10^{11} Pa$, $G = 2.7 * 10^{10} Pa$, $J = 118.3261$, $\rho = 2770 \frac{kg}{m^3}$, $l = 0.9144 m (26")$, and $N = 90$ elements. The reason that there were only 90 elements was due to the processing restriction in ANSYS only allowing an element size of 0.02m. J is the torsional constant that was calculated assuming the airfoil was an ellipse using Equation (5).

$$J \triangleq \frac{\pi a^3 b^3}{a^2 + b^2} \quad (5)$$

A new variable was defined: $L = \frac{l}{N}$. This divided up the length of the bar into the previously defined elements. The second moment of inertias, I_{xx} , I_{yy} , and I_{zz} , of the Alouette rotor was calculated in PTC Creo using the cross-section properties analysis tool seen in Fig. 18. PTC Creo's measuring tool was also used to get the cross-sectional area of the model.

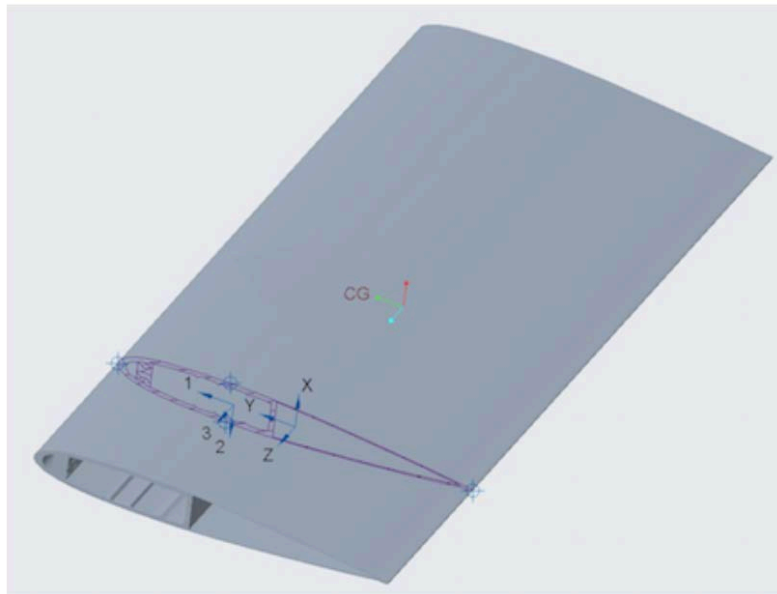


Figure 18: PTC Creo's Cross Section view used to calculate the Second Moment of Area

3. Matrix Set Up

To get a better understanding on how to simulate the model in MATLAB, Euler-Bernoulli Beam Theory was applied¹⁶. This gave the mass and stiffness matrix defined in Equations (6) and (7) respectively for the X and Z axis.

$$K = \frac{EI_x}{L^3} \begin{bmatrix} 12 & 6L & -12 & 6L \\ 6L & 4L^2 & -6L & 2L^2 \\ -12 & -6L & 12 & -6L \\ 6L & 2L^2 & -6L & 4L^2 \end{bmatrix} \quad (6)$$

$$M = \frac{\rho AL}{420} \begin{bmatrix} 156 & 22L & 54 & -13L \\ 22L & 4L^2 & 13L & -3L^2 \\ 54 & 13L & 156 & -22L \\ -13L & -3L^2 & -22L & 4L^2 \end{bmatrix} \quad (7)$$

Since the Euler Bernoulli matrices apply to each element, an algorithm was then executed to construct the overall mass and stiffness matrices. The first step of the algorithm was to generate the $2N \times 2N$ matrix with the end elements. A separate algorithm was then applied to combine each element forming the overall mass and stiffness matrix of the beam. Then, the boundary conditions, $v = 0$ and $\phi = 0$, on the fixed end were applied for the cantilevered beam.

For the Y axis, a torsional spring stiffness matrix was used seen in Equation (8). For the mass matrix, Equation (9), Variational Mass Lumping was used because it preserves linear momentum along the Y axis and angular momentum about the X axis.

$$K = \frac{GJ}{L} \begin{bmatrix} 1 & -1 \\ -1 & 1 \end{bmatrix} \quad (8)$$

$$M = \frac{\rho AL}{6} \begin{bmatrix} 2 & 1 \\ 1 & 2 \end{bmatrix} \quad (9)$$

4. Results

Since we are looking for the solution of an undamped free vibration problem, it is the same as an eigenvalue problem. The eigenvalue solver in MATLAB was used and the eigenvalue and corresponding eigenvector was calculated. We can ignore any modes that appear above 600 Hz since we are using the MIL-STD810F standard, which is the United States Military Standard that tests the limits to the conditions and environments that the test unit will experience throughout its service life. The results can be seen in Appendix A and Table 2 and Fig. 8 below.

Table 2: MATLAB Results for the Alouette Rotor

<u>Mode</u>	<u>Frequency (Hz)</u>	<u>Axis of Rotation</u>
1	14.86	X
2	93.13	X
3	97.36	Z
4	260.77	X
5	511.01	X
6	86251.10*	Y

*Torsional bending moment about Y discussed in section V.

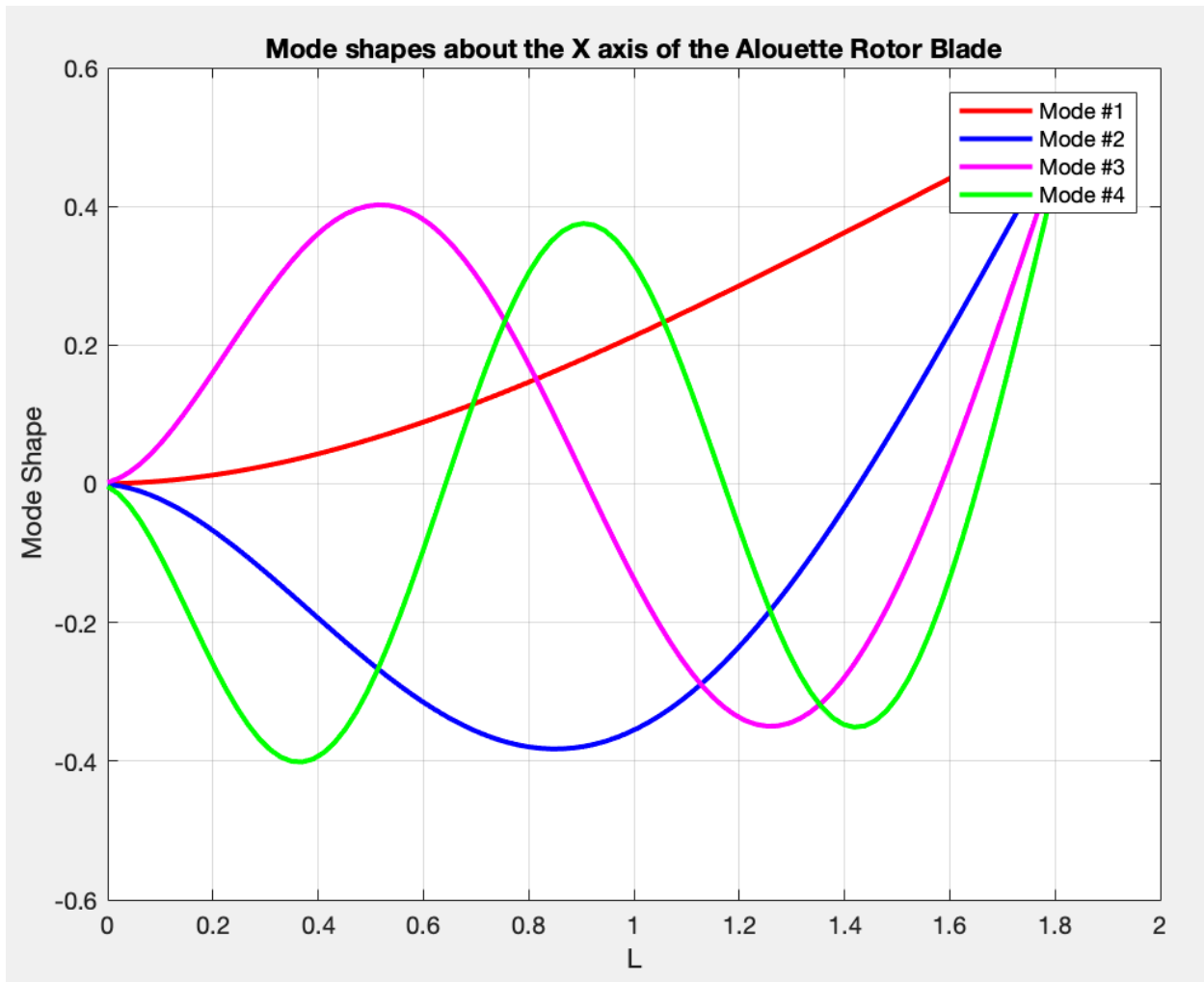


Figure 19: Mode Shapes about the X Axis

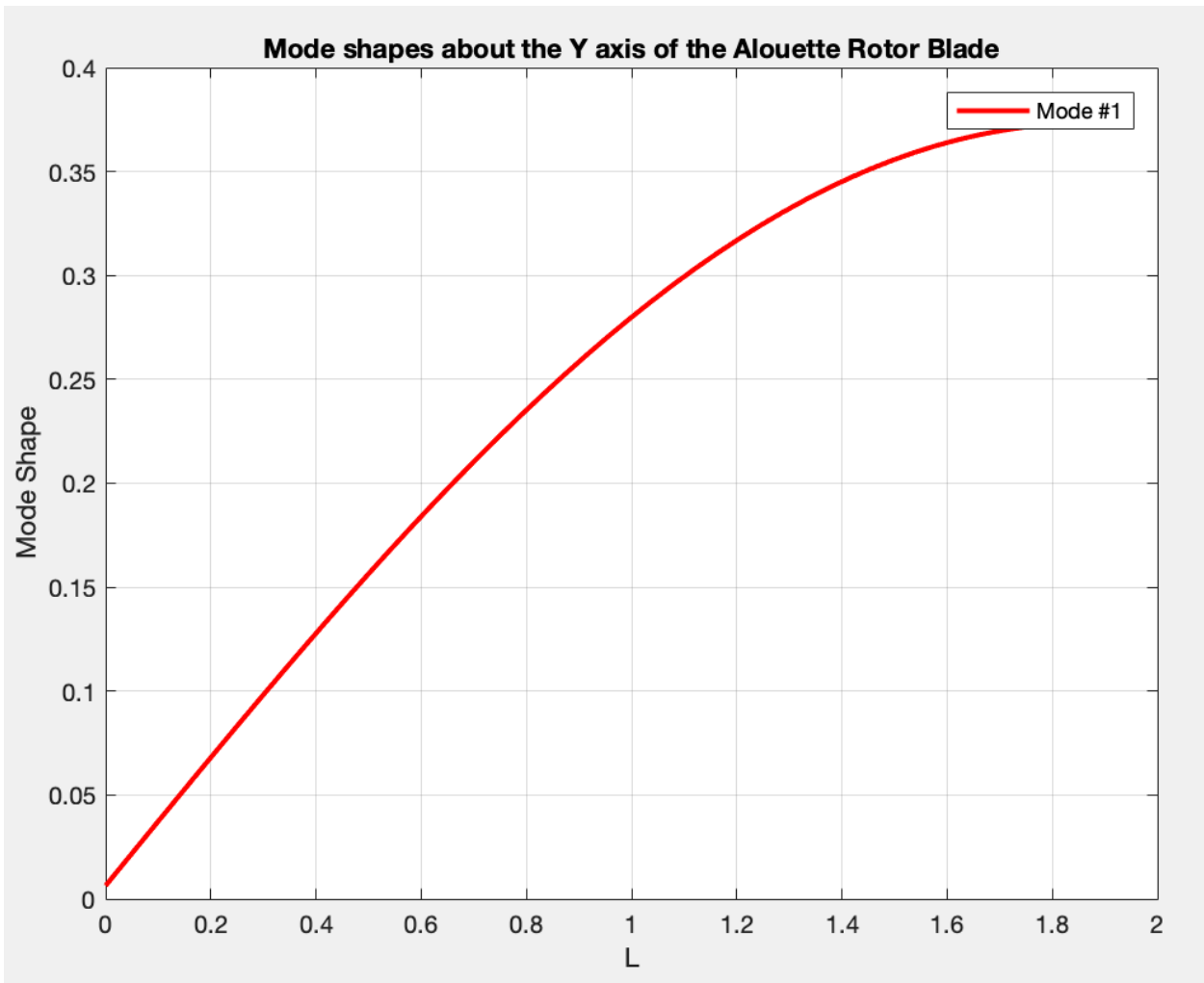


Figure 20: Mode Shapes about the Y Axis

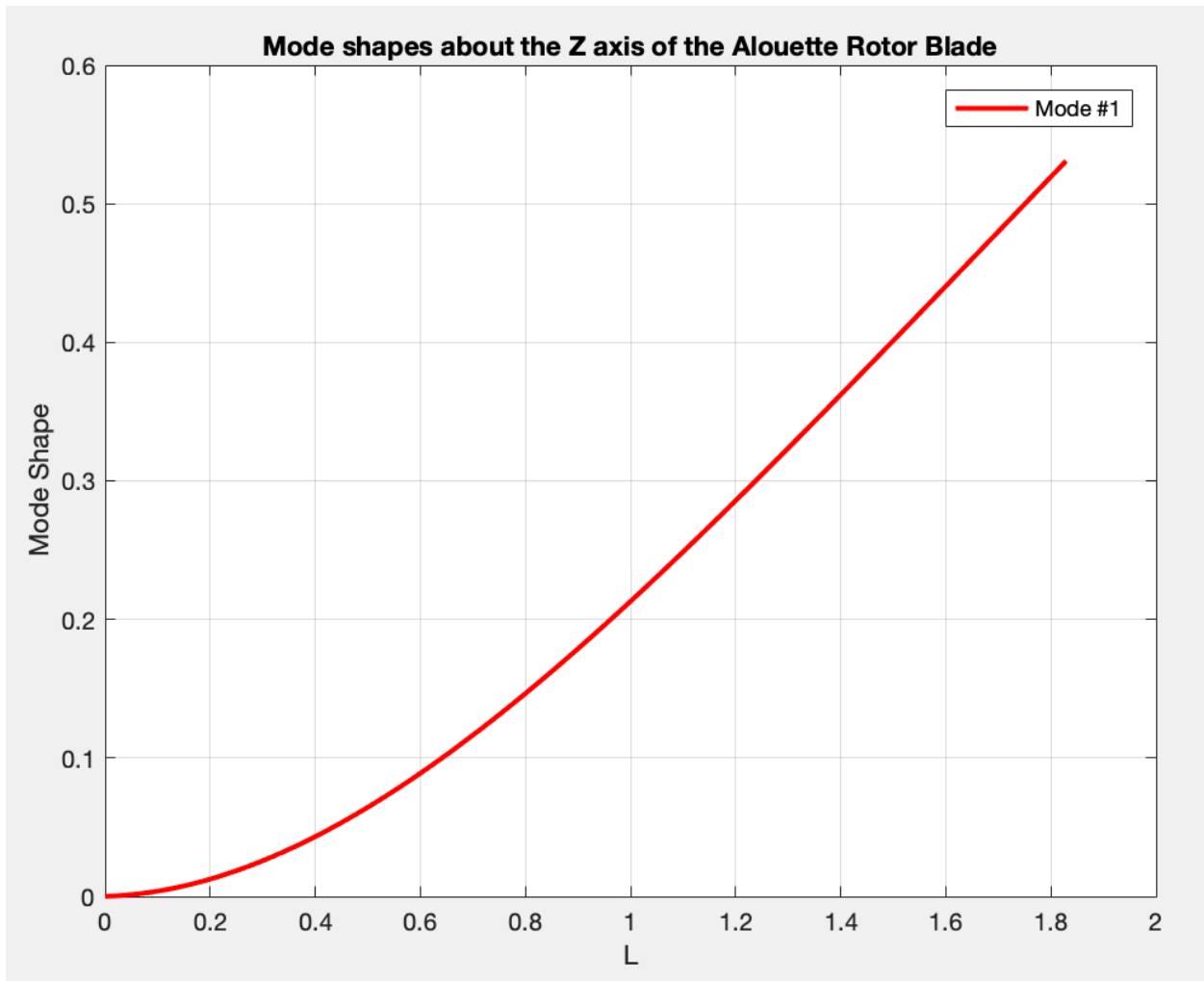


Figure 21: Mode Shapes about the Z Axis

III. Testing

A. Test Set Up

The test was performed at Lockheed Martin in Building 156G in Test Stand 1. The test stand has been built with a 90-foot foundation in order to minimize noise generated from outside of the cell. The test stand has I-beams already placed throughout the stand in order to mount test fixtures or hang units under test. In the cells, there are two cranes capable of craning 10 tons and one in the test stand can be seen in Fig 22.

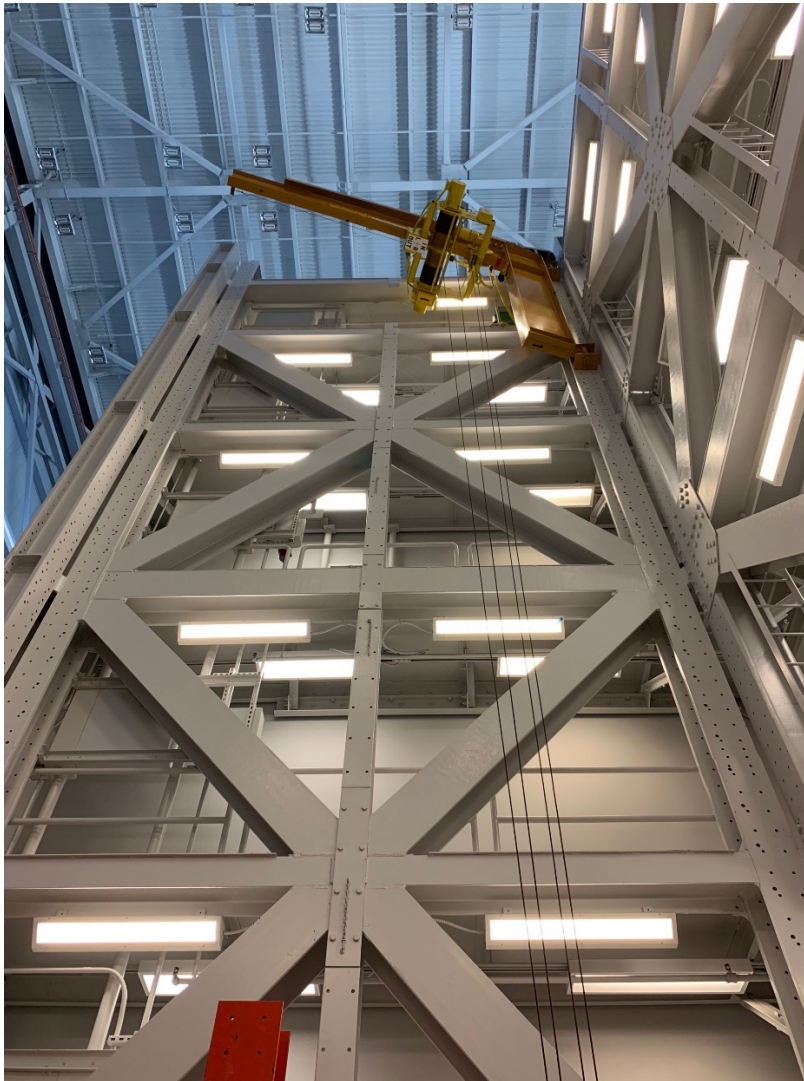


Figure 22: Test Stand 1 crane

1. Data Acquisition System

The data acquisition and control systems were made by Agilent. 1 chassis holds 1 MXIbus to VXI communication card, 1 Agilent E1434A 4-channel signal source card, and 11 Agilent E1432A 16 channel acquisition cards were used in the mainframe. Another component in the mainframe is a Krown-Hite Corporation filter configured into a low pass filter that allowed 600Hz and below along with an ICP signal conditioner. There was also an oscilloscope used to view if the signal was being transmitted out from the source card that was connected to a power amplifier. The power amplifier then boosted the signal to the shaker. A picture of the mainframe can be seen below.

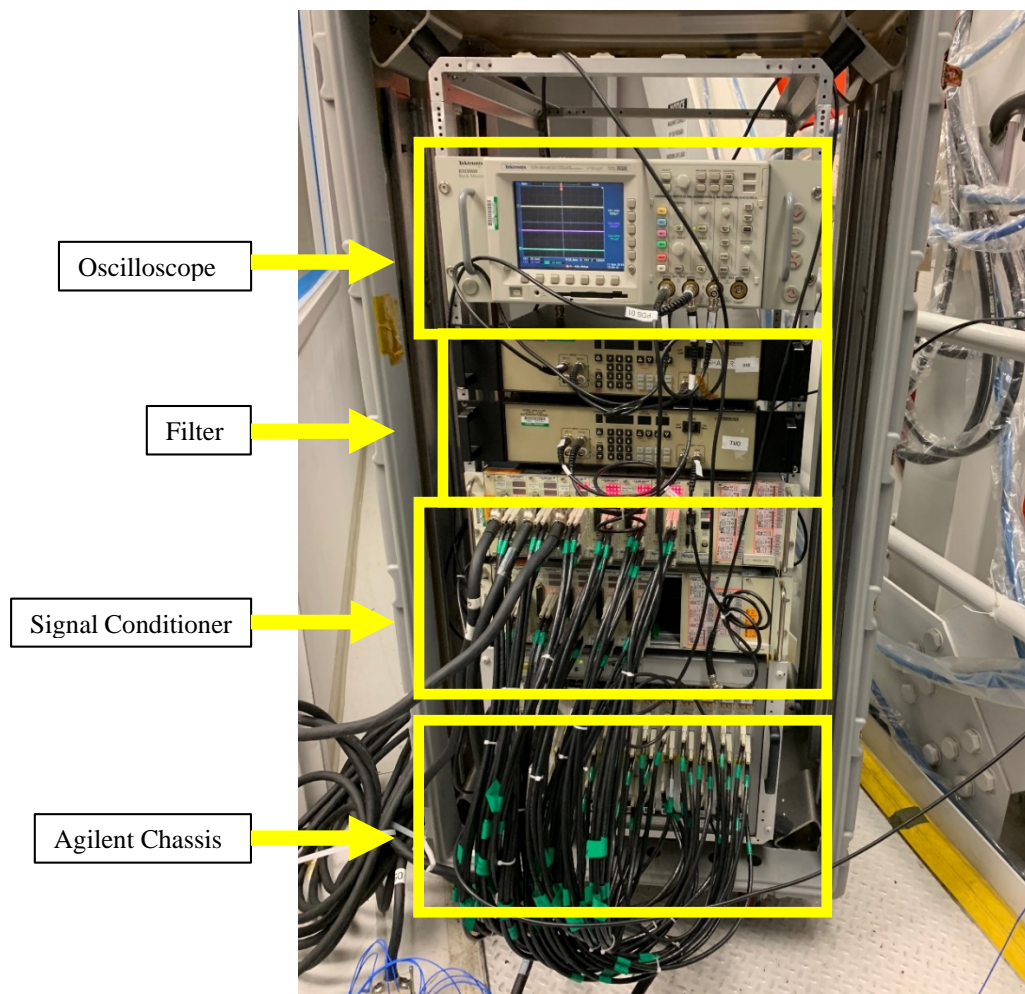


Figure 23: DAS Mainframe

2. Shakers

The model of the shaker used was the MB Dynamics model MB25 with a 10 lbf_{pk} and a 0.5” stroke. The shaker was hung off of the crane, connected to a lifting sling, connected to a shackle, connected to 3 individual bungies for isolation, and 3 turnbuckles to have control over the angle the shaker is facing. The shaker was then angled 45° so that the energy would be input at (45°, -45°, -45°) off of the left tip. This excitation angle was chosen because it would excite all axes of the unit under test (UUT). The shaker was connected to an impedance head that doubles as a load cell and an accelerometer.

Another excitation method that was used was the modal hammer. The modal hammer functions as an impulse to the system. The frequency content of the energy applied to the UUT is a function of the stiffness of the contacting surfaces and the mass of the hammer. With this in mind, the soft tip was used for better low frequency content since we are limiting our bandwidth to 600 Hz.



Figure 24: Modal Hammer

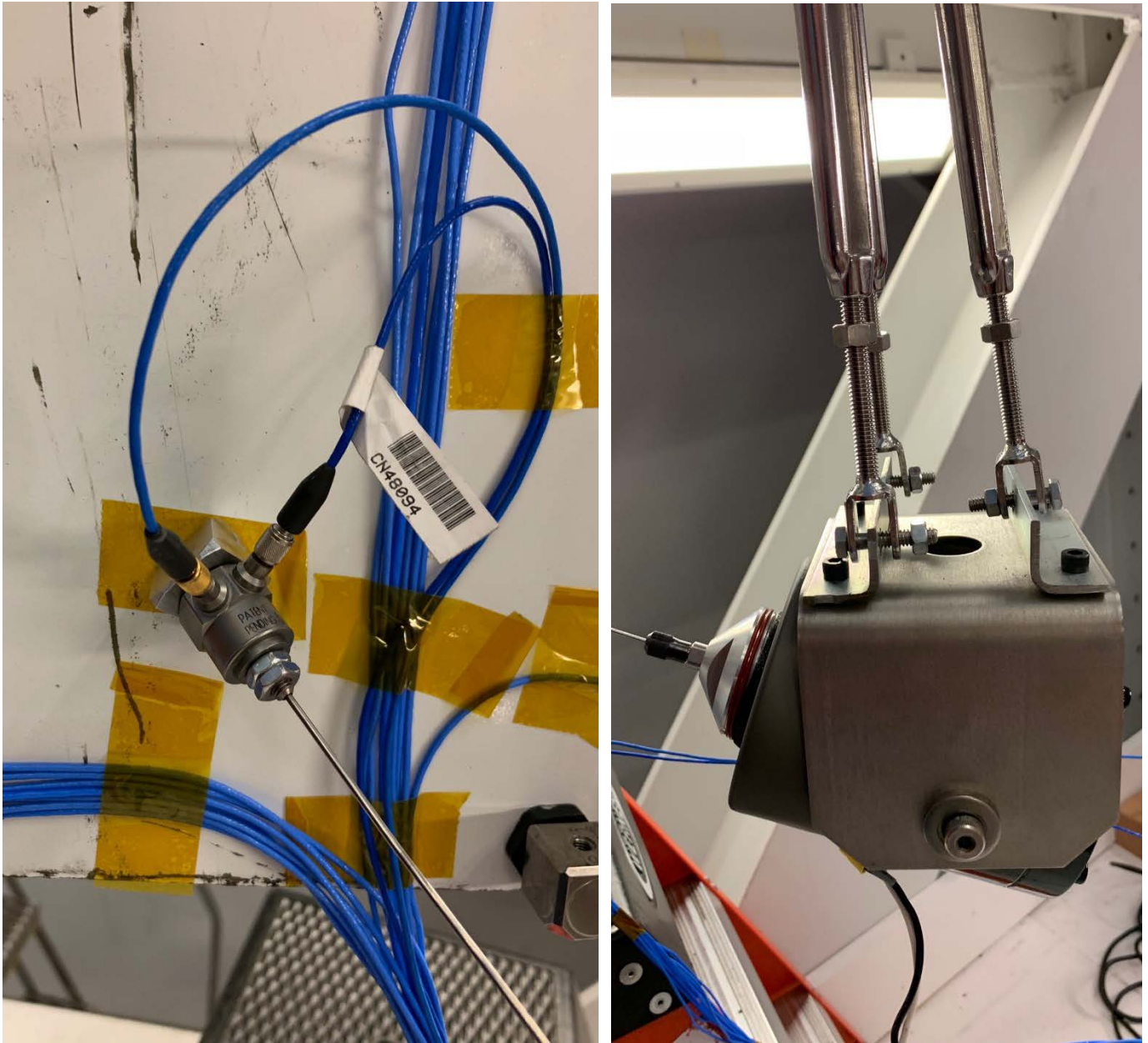


Figure 25: Modal Shaker (right) w/ impedance head (left)

3. Accelerometers

The locations of the accelerometers were determined using two methods. The first method was evaluating where the highest deformation would occur. The second method is to look at which area have the most moving mass. This means that even though there is not a high reaction at those locations, it is involved in the other different mode shapes. Using these two criteria, it was determined that a total of 14 accelerometers would be needed. 7 on the leading edge and 7 on the trailing edge. These accelerometers were triaxial, which means that each sensor has 3 axes is can measure.

Since the first mode was estimated to be in the 15 Hz range, the accelerometers chosen were 10 PCB T256M98's and 4 PCB 356B18's. These accelerometers are calibrated in the 5Hz-3000Hz range and have a sensitivity of around 1000 mV/g. The force gages on the modal hammer and the shaker have the sensitivity of 10 mV/lb.

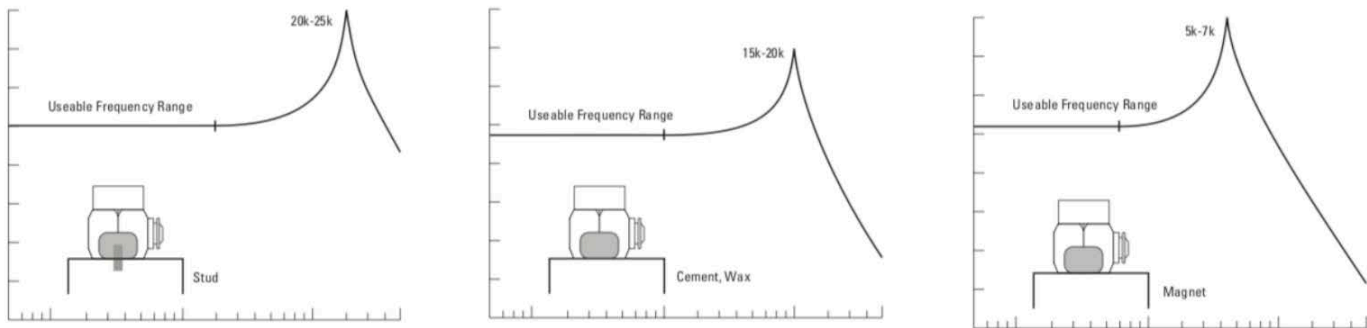


Figure 26: Three methods to mounting an accelerometer

There are three ways to mount accelerometers. The first way is to mount the accelerometer is to physically screw the sensor into the UUT. This provides the highest usable frequency range of the 3 options, however, it requires making modifications onto the test article. This type of invasive mounting technique is usually not done, especially if it is flight hardware due to damaging and the time necessary to implement this method. The second type is a cement or wax technique. These

types of bond have a usable frequency range up to 15k-20k Hz. This method is faster to mount and leaves minimal marks but it does take some time to mount. The last method is a magnet, which has the lowest usable frequency range of 5k-7k Hz. This method only requires the surface of the UUT to be magnetic.

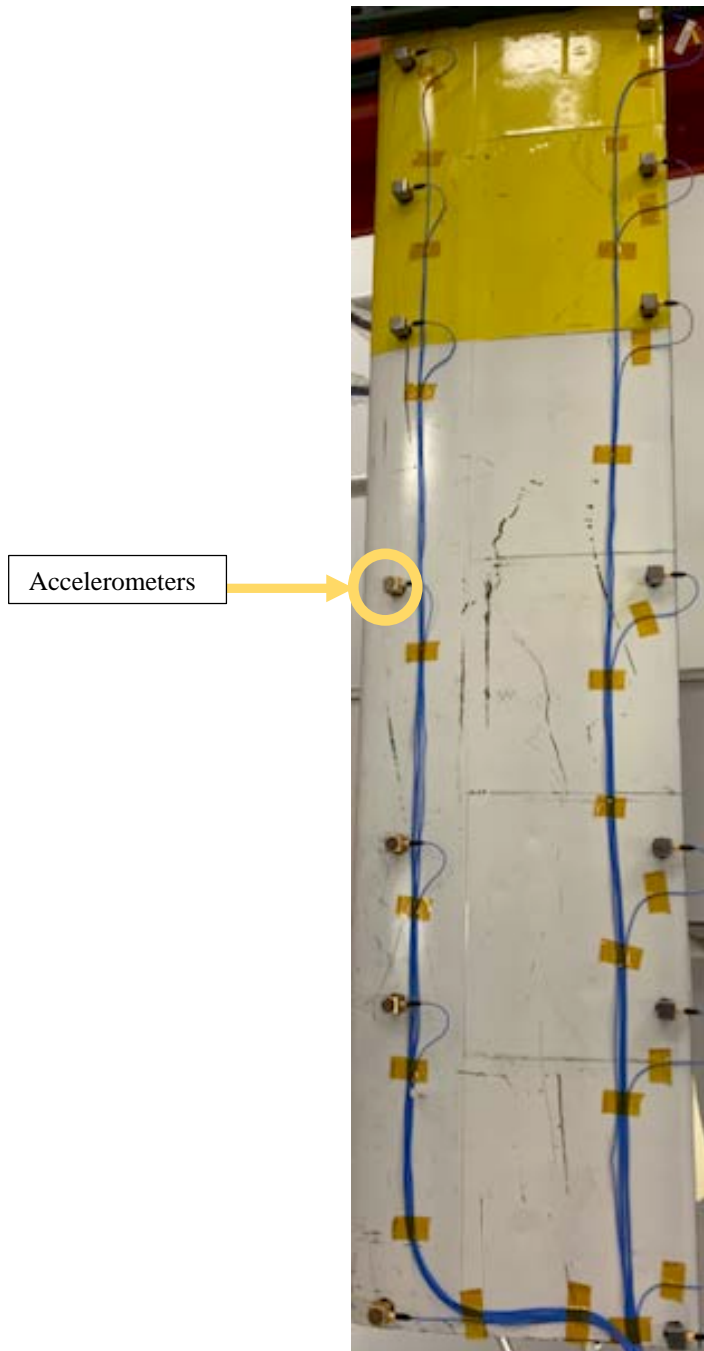


Figure 27: Accelerometer Locations

B. Test

The test article is configured as a cantilever beam. This was accomplished by mounting the rotor blade onto the I-beam through the use of Unistrut, effectively clamping down one end. The orientation of the accelerometers shown has the X-axis to the left of photo, Y-axis is down the span of the rotor blade, and the Z-axis is towards the camera. In the software, the Y and Z axis are changed to mimic the coordinate system in the ANSYS simulation.

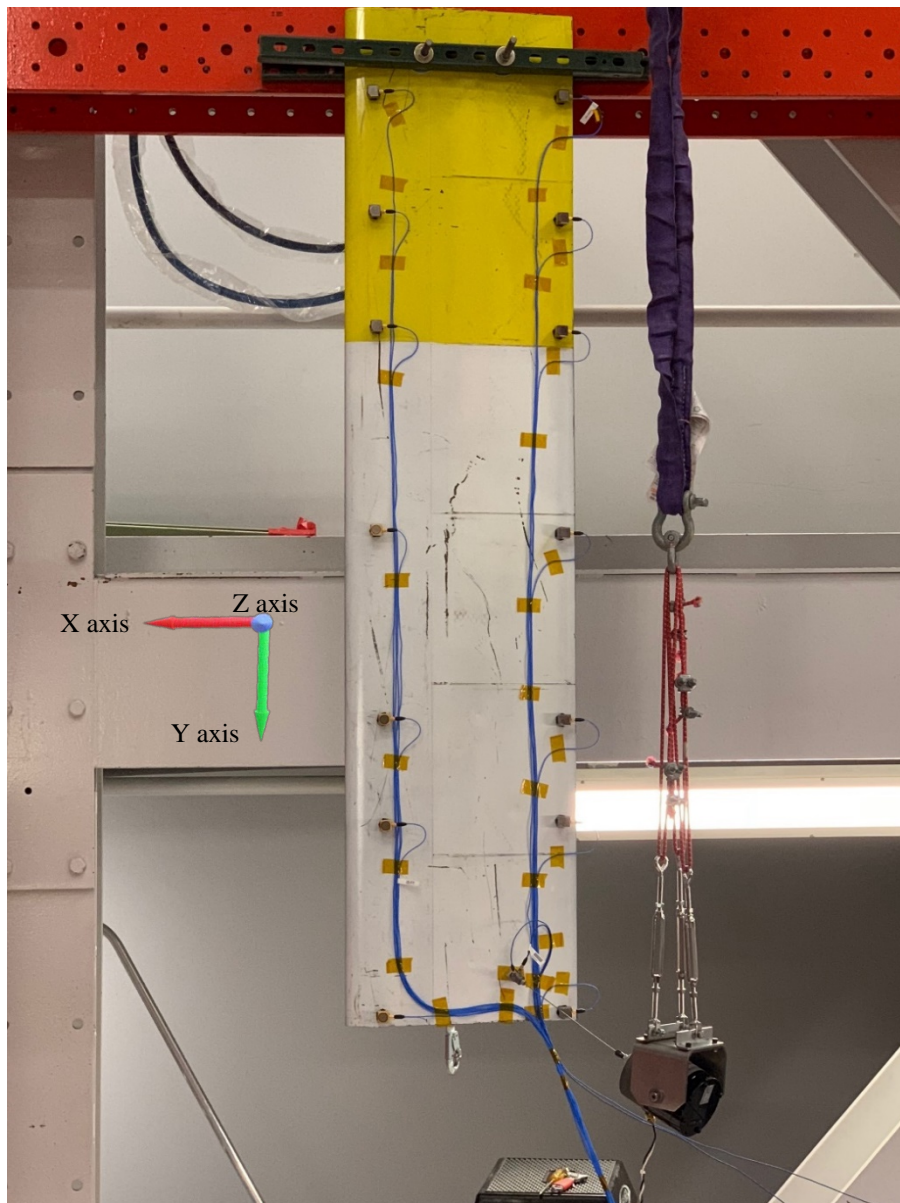


Figure 28: Test set up with the modal shaker hanging from the crane

When using the shaker, a burst random signal was used with an 80% on and 20% off. This allowed the UUT to settle down in time for the next burst sine. The frequency bound was 0 Hz-640 Hz and the low pass filter only allowed 600 Hz and below through to the shaker. The force levels used were 1 pound and 1.25 pounds respectively to show linearity in the mode shapes.

The sample frequency used was 8192 Hz due to Eqn. 10. The frame length was 5 seconds with a bandwidth of 600 Hz gives us a sample frequency of ≥ 6000 Hz to eliminate aliasing. It is far better to over sample than under sample and get erroneous readings, especially since memory space has now become so readily available. A total of 5 samples per run were used with a manual trigger. This means that the Test Conductor has to signal to the computer to begin sending the signal. This ensures that the UUT has come completely to rest. A time history sample can be found in Fig. 29.

$$\text{sample frequency} \geq 2 * \text{bandwidth} * \text{time} \quad (10)$$

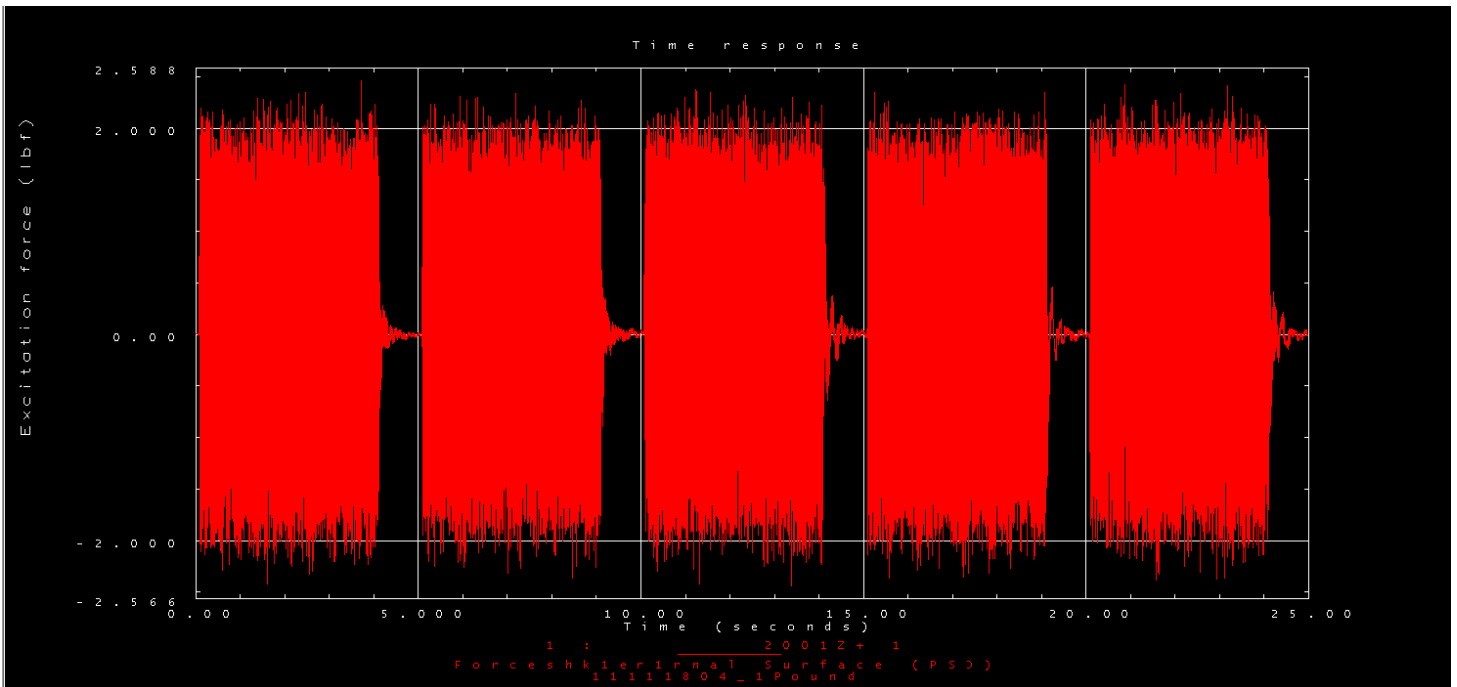


Figure 29: Time history plot of force of the shaker

NX Test For Ideas was used as the data acquisition software. It is able to produce time histories for every sensor as seen in Fig. 29. It can also generate frequency response functions (FRF) seen in Fig. 30. These are considered preprocessed data. The test conductor will reference the time histories to confirm the levels and health of the test. The test conductor can also use the FRF plots generated to get a preliminary estimation on where the modes are located. The modes are visible because there is a much higher response at certain frequencies.

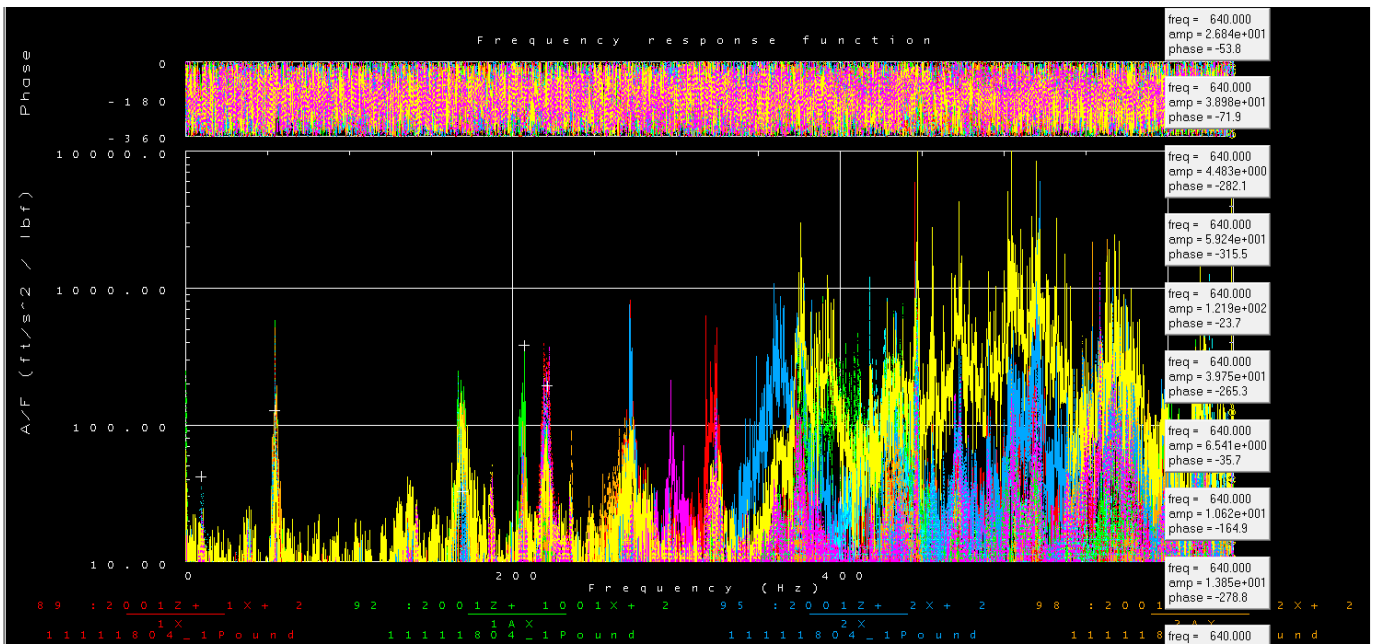


Figure 30: FRF generated by NX Test For Ideas

C. Results

Using NX Test for Ideas, a post processing application was used called AFpoly. This takes the data and creates a power spectral mode indicator functions (PSMIF) seen in Fig 31, Fig 32, and Fig 33. This displays the processed shape data captured in NX Test for Ideas. From this, the Test Conductor is able to set the range of the frequency to be evaluated, the reference signal, the response signals, and the poly modal options. The Auto Select Poles option is used in the poles tab. The results can be seen below.

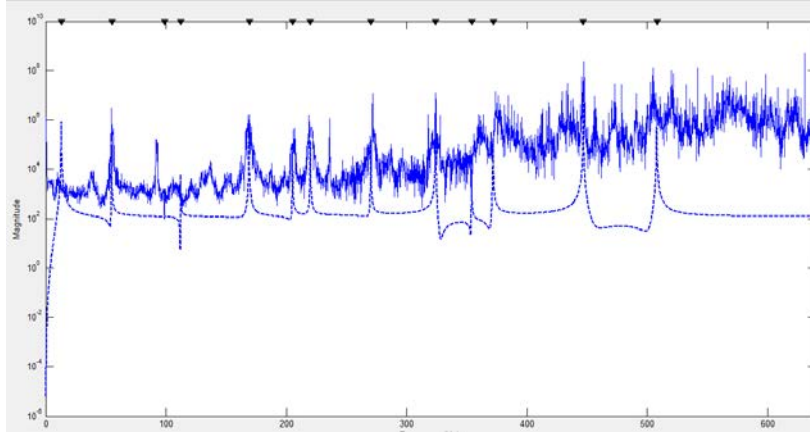


Figure 31: PSMIF for the 1 pound RMS run

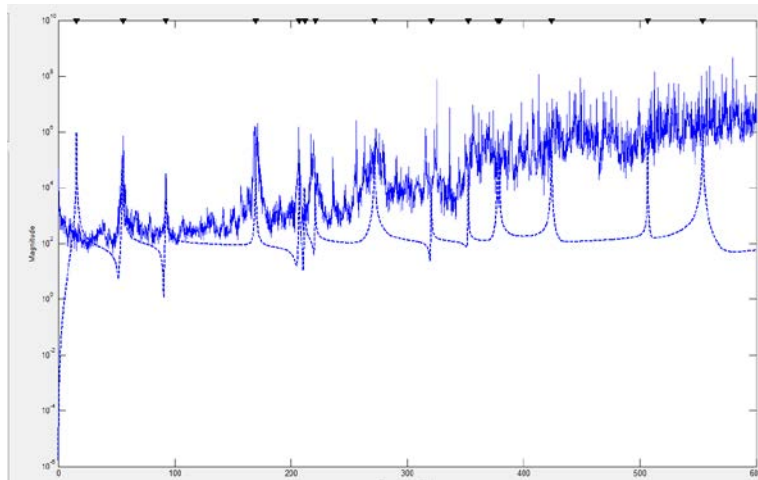


Figure 32: PSMIF for the 1.25 pounds RMS run

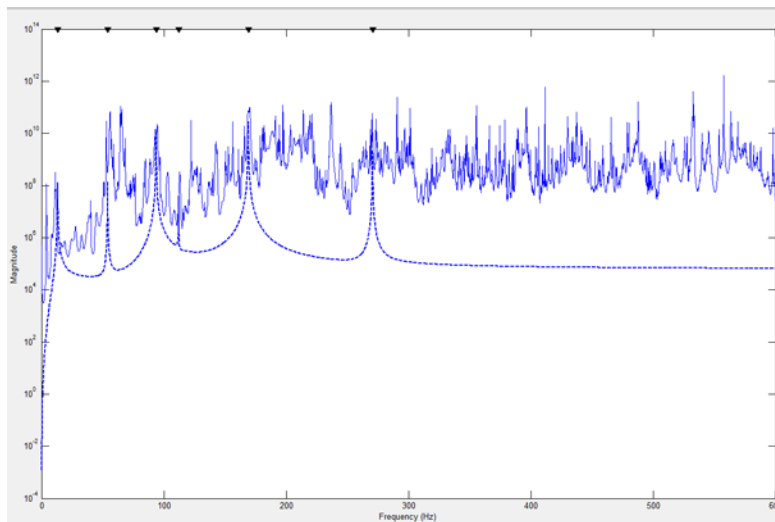


Figure 33: PSMIF for the tap test with the modal hammer

The PSMIF shows the general mode shape frequencies processed from the data. The modes can be seen as the large spikes above the noise floor. The dotted line is the function generated from the auto selecting of the poles. It is important to note that multiple runs at the same level were performed to prove repeatability. The modes that were found in AFPoly, and confirmed through multiple runs, are tabulated into Table 3 below.

Table 3 Modal Test results for Alouette rotor blade

<u>Mode</u>	<u>Frequency (Hz)</u>	<u>Force Level Shape Was Found</u>
1	13.07	1.00 lbf
2	54.96	1.00 lbf
3	92.28	1.25 lbf
4	98.78	1.00 lbf
5	112.15	1.00 lbf
6	169.11	1.00 lbf
7	205.24	1.00 lbf
8	270.36	1.00 lbf
9	324.15	1.00 lbf
10	354.02	1.00 lbf
11	371.83	1.00 lbf
12	424.06	1.00 lbf
13	507.87	1.00 lbf

IV. Error Analysis

A. MATLAB

As previously stated, the same parameters were used in the MATLAB code as in ANSYS. One end was defined as a fixed support and no load was applied. The number of elements was the same in the y direction as the code. The one difference would be that there are elements in the x and y direction to account for the 3-dimensional analysis versus the three 1-dimensional analysis provided by the MATLAB code. Another would be that the MATLAB code used a square mesh versus the combination of tetrahedrons and pyramids used in the 3D mesh in ANSYS. Also, the

MATLAB code is applying Euler Bernoulli beam theory while ANSYS implements Timoshenko beam theory by default. Timoshenko beam theory, unlike Euler Bernoulli beam theory, accounts for transverse shear strains. This means that the Euler-Bernoulli element is 'stiffer' and can lead to the percent error increasing at the higher modes. Another reason for the differences can be due to the meshing in ANSYS. The 'mesh' used in the MATLAB simulation only broke the model up into equal length elements along the span while ANSYS used a combination of tetrahedrons and pyramids. The MATLAB code used linear approximations with Euler Bernoulli beam theory instead of a more accurate nonlinear relationship. This would explain why the mode shapes around the Y axis were difficult to calculate. Using these simplifications resulted in the first torsional mode to be placed at 86251.10 Hz. This is not the case because both ANSYS and MATLAB had the first torsional mode ~98 Hz.

B. ANSYS

ANSYS was set up to mimic the test configuration in Test Stand 1. One end was defined as a fixed support, modeling one end of the rotor blade clamped to the I-beams around the test stand. One thing to note was that the airfoil's skin was not modeled correctly. When performing the test set up, it was found that the airfoil had a thin layer of aluminum that was wrapped around some Styrofoam, which then had another aluminum sheet wrapped around that to make up the skin.

C. Testing

This comparison is where the most deviation was expected to occur. One of the errors from testing could be that the rotor blade was not fixed tightly on one end. Another would be that the shaker was not secured tightly onto the test article. Halfway during the testing phase, there was a weird sound coming from the set up. It was discovered that collet that connects the shaker to the impedance head was loose, and the shaker was not putting in as much energy into the system as it

was believed. The shaker collet was tightened, and the runs were rerun in order to obtain clean data. Also, if the shaker was not directly in line with the mounting point, it could impart extra unwanted moments onto the test article. Another error could come from not changing the position of the excitation source. This was mitigated by using a modal hammer to make sure that all axes were excited. The only drawback is that the hammer is only good for low frequency content.

V. Conclusion

A. ANSYS vs MATLAB

Table 4 ANSYS results versus MATLAB results

Mode	ANSYS Frequency (Hz)	MATLAB Frequency (Hz)
1	15.34	14.86
2	92.25	93.13
3	97.446	97.36
4	125.09	----
5	244.05	260.77
6	348.09	----
7	443.62	511.01
8	488.35	----
9	528.24	----

It is shown that the first mode shape was fairly close between the simulations. The MATLAB simulation provided 14.86 Hz, while ANSYS gave 15.34 Hz, resulting in a 3.1% error between the two. The next mode shape resulted in less error at .95% error, which was expected since the percent error continues to grow in the case of Euler Bernoulli beam theory as the frequencies increased. The rest of the mode shapes about the X axis grew to 6.9% and 15.2% respectively, which is to be expected due to the assumptions and simplifications made when using Euler Bernoulli Theory. The modes about the Z axis was accurate for the first mode at .1% error. However, the second mode grew to 24.9% error and the MATLAB code gave it to be 610.14 Hz,

just outside our bandwidth. Our modes about the Y axis will be discussed in Section V. One thing to note was that the mode shapes themselves were similar between MATLAB and ANSYS.

B. Testing vs ANSYS

Table 5 Testing results versus ANSYS results

<u>Mode</u>	<u>Testing Frequency (Hz)</u>	<u>ANSYS Frequency (Hz)</u>
1	13.07	15.34
2	54.96	----
3	92.28	92.25
4	98.78	97.446
5	112.15	125.09
6	169.11	----
7	205.24	----
8	270.36	244.05
9	324.15	----
10	354.02	348.09
11	371.83	443.62
12	424.06	488.35
13	507.87	528.24

The first mode shape, about the X axis, had a large error of 17.4%. When the results were in, the 1.25 lbf run actually found the mode shape to be 15.64 Hz. This would have resulted in only a 1.9% error. However, the tap test data also found the first mode shape to be at 13.32 Hz. After that, a similar trend occurred much like the ANSYS vs MATLAB comparison. The next modes had a .03%, 9.73%, and 19.31% error for each sequential mode about the X axis (modes 3, 8, and 11). Interestingly enough, the same thing happened with the modes about the Y axis where the largest % error happening in the first mode at 11.53% error for mode 5. After that, it followed the same trend where the % error grew for each mode after that about the Y axis at 1.68% and 4.01% error for modes 10 and 14. The Z axis was the only axis not to exhibit the same trend where the

first mode was off by a large margin. It did show the same trend where the % error increased as the mode shapes progressed at 1.35% and 15.16% error for modes 4 and 13.

C. Testing vs MATLAB

Table 6 Testing results versus MATLAB results

<u>Mode</u>	<u>Testing Frequency (Hz)</u>	<u>MATLAB Frequency (Hz)</u>
1	13.07	14.86
2	54.96	----
3	92.28	93.14
4	98.78	97.36
5	112.15	----
6	169.11	----
7	205.24	----
8	270.36	260.79
9	324.15	----
10	354.02	----
11	371.83	511.04
12	424.06	----
13	507.87	----

The first mode shape was about the X axis, and like the X axis with the ANSYS comparison, had a large difference at 13.70% error. It then followed the same trend where the percent error fell to .93%, then grew to 3.54%, and finally had a 20.51% error for modes 3, 8, and 11 about the X axis. The modes about the Z axis had a 1.43% error and 20.14% error respectively for modes 4 and 13. Like previously stated in the ANSYS vs MATLAB comparison, MATLAB calculated the second mode shape about the Z axis at 610.14 Hz, which is outside of the range set by the MIL-STD810F standard.

This project successfully simulated most of the mode shapes for an Alouette rotor blade through a MATLAB code and a professional engineering software package. Obviously, ANSYS did a

much better job simulating the mode shapes because it allows the user to not make as many assumptions and simplifications. ANSYS is a powerful tool that allows a person to model, mesh, and solve complex problems that would be difficult and time consuming to execute using MATLAB alone. An important thing to note when using any software package is that problem is fully defined correctly, the correct boundary conditions are implemented, and the appropriate material approximations are made. The most important thing to remember as an engineer is to evaluate the results to ensure that the results are feasible.

References

- ¹Chentao Li, Shuqian Fan and Mingquan Shi, "Preparation of CAD model for finite element analysis," *2010 International Conference on Computer, Mechatronics, Control and Electronic Engineering, Changchun*, 2010, pp. 491-494.
- ²Svoboda, F., and Hromcik, M. "Finite Element Method Based Modeling of a Flexible Wing Structure," *2017 21st International Conference on Process Control (PC)*, Strbske Pleso, 2017, pp. 222-227.
- ³Mitiguy, P. "Dynamics – what does it do for us?" *Dynamics of Mechanical, Aerospace, and Biomechanical System*, Student Edition, 2014, pp. i-ii.
- ⁴Kelly, S. "Basic Principles of Rigid-Body Kinetics for Planar Motion" *Fundamentals of Mechanical Vibrations*, 2nd Edition, McGraw-Hill, New York, 2000, pp. 11-13.
- ⁵Lim, J., Hwang, D.S., Kim, K.W., Lee, G., Kim, J.G., "A coupled dynamic loads analysis of satellites with an enhanced Craig–Bampton approach," *Aerospace Science and Technology*, Vol. 69, 2017, pp. 114-122,
- ⁶Craig Jr, R. and Bampton, M., "Coupling of substructures for dynamic analyses." *AIAA Journal*, Vol. 6, No. 7 (1968), pp. 1313-1319.
- ⁷Shabana, A., "An Absolute Nodal Coordinates Formulation for the Large Rotation and Deformation Analysis Of Flexible Bodies," Report.No.MBS96–1-UIC, University of Illinois at Chicago, 1996.
- ⁸Sun, J.L., Tian, Q., Hu, H.Y., "Structural Optimization of Flexible Components in a Flexible Multibody System Modeled Via ANCF," *Mechanism and Machine Theory*, Vol 104, 2016, pp. 59-80.
- ⁹Luo, K., Hu, H.Y., Liu, C., Tian, Q., "Model Order Reduction for Dynamic Simulation of a Flexible Multibody System Via Absolute Nodal Coordinate Formulation," *Computer Methods in Applied Mechanics and Engineering*, Vol. 324, 2017, pp. 573-594,
- ¹⁰Wang, Z., Tian, Q., Hu, H.Y., "Dynamics of Spatial Rigid Flexible Multibody Systems with Uncertain Interval Parameters," *Nonlinear Dynamics*. 84, 2016, pp. 527–548.
- ¹¹Simmons, R., "MOLA Mechanical Analysis Home Page", *MOLA Analysis Documents, Pictures, and Information* [online database], <https://analyst.gsfc.nasa.gov/ryan/MOLA/moladocs.html>, 2002.
- ¹²Cusano, A., Capoluongo, P., Campopiano, S., Cutolo, A., Giordano, M., Felli, F., Paolozzi, A., Caponero, M., "Experimental modal analysis of an aircraft model wing by embedded fiber Bragg grating sensors," *IEEE Sensors Journal*, Vol. 6, 2006, pp. 67-77.
- ¹³Hunter, J., "Alouette Rotor Blade," Apr. 2013.
- ¹⁴United States Department of Defense, "TEST METHOD STANDARD: ENVIRONMENTAL ENGINEERING CONSIDERATIONS AND LABORATORY TESTS", *United States Department of Defense*, MIL-STD-810F, 2003
- ¹⁵Wang, E., and Nelson, T., "Structural Dynamic Capabilities of ANSYS," ANSYS, Inc. Irvine, CA
- ¹⁶Felippa, Carlos, "Advanced Variational Methods In Mechanics", *University of Colorado at Boulder*, Chapter 16 <https://www.colorado.edu/engineering/CAS/courses.d/AVMM.d/>
- ¹⁷Logan, D., *A First Course in the Finite Element Method*, Stamford, CT: Global Engineering, 2012.